Reversal of Polymerization Stereoregulation in Anionic Polymerization of MMA by Chiral Metallocene and Non-metallocene Initiators: A New Reaction Pathway for Metallocene-Initiated MMA Polymerization

Andrew D. Bolig and Eugene Y.-X. Chen*

Department of Chemistry, Colorado State University Fort Collins, Colorado 80523-1872

Received May 13, 2001

Cationic group 4 metallocene and related complexes have attracted increasing attention from both academia and industry because they are structurally well-defined, typically highly active, single-site olefin polymerization catalysts which produce polyolefins with controlled microstructures.[1] The ultimate and largely unmet challenge in this field, however, is the discovery of new catalytic systems for the controlled polymerization of polar functional monomers and copolymerization of these monomers with simple olefins.[2] Noteworthy successes in this regard include the discoveries by Collins et al.[3] and Yasuda et al.[4] that zirconocenes[5−7] and lanthanocenes[8] are efficient initiators for the controlled homopolymerization of methacrylic monomers, particularly methyl methacrylate (MMA). Either a neutral metal (Zr or Sm) enolate or a cationic Zr enolate is believed to participate in the propagation with a mechanism analogous to group-transfer polymerization (GTP).[9] We communicate here a new reaction pathway for metallocene-initiated MMA polymerization using zirconocenium aluminates as well as an efficient synthesis of highly syndiotactic PMMA through enolaluminate formation and monomer activation with tris(pentafluorophenyl)alane.

Polymerization of MMA using chiral zirconocenium cations paired with weakly coordinating borate anions derived from C_2-symmetric *ansa*-zirconocenes produces highly isotactic PMMA via an enantiomorphic-site control mechanism.[5b,e,6c,d,f,g] In sharp contrast, polymerization of MMA using the same zirconocenium cation, but paired with an aluminate anion, affords syndiotactic PMMA (Table 1). As can been seen from the table, *rac*-(SBI)-$ZrMe^+MeB(C_6F_5)_3^-$ (**1**, SBI = $Me_2Si(\eta^5\text{-Ind})_2$)[10] produced isotactic PMMA (%[*mm*] = 92.7) (run 1). The triad distribution is consistent with a site-control mechanism (2[*rr*]/[*mr*] = 1.1). Unexpectedly, use of *rac*-(SBI)$ZrMe^+MeAl(C_6F_5)_3^-$ (**2**)[11] produced syndiotactic-rich PMMA (runs 2 and 3). Triad tests suggest that the stereochemistry of the polymerization is predominately chain-end controlled (4[*rr*][*mm*]/[*mr*]^2 = 0.8 and 0.9 for runs 2 and 3, respectively). Consistent with syndiotactic microstructures, PMMAs produced by **2** have T_g values of 112.5 and 127.1 °C at T_p of 23 and 0 °C, which are considerably higher than that of isotactic PMMA produced by **1** (T_g = 55.9 °C). Polymerizations by **1** and **2** are well-controlled even at ambient polymerization temperature, affording PMMAs with narrow molecular weight distributions of 1.12−1.32. Control runs using *rac*-(SBI)$ZrMe_2$ (**3**) or Lewis acids $M(C_6F_5)_3$ (M = B, Al) alone did not produce any isolable polymers under the same polymerization conditions.

Evidence that the MMA polymerization by zirconocenium aluminates undergoes a different mechanism involving enolaluminates derives from several lines. First, the polymerization of MMA was followed in NMR-scale reactions with both ^{1}H and ^{19}F NMR being monitored from −40 °C to room temperature. In MMA polymerization initiated by **1**, ^{19}F NMR spectra revealed that the initial weakly coordinated anion $MeB(C_6F_5)_3^-$ in **1** became a free, noncoordinated anion[12] after addition of MMA which remained unchanged throughout the polymerization (Figure 1), consistent with the polymerization mechanism involving a cationic zirconocene enolate.[5,6] In sharp contrast, for MMA polymerization initiated by **2**, the $MeAl(C_6F_5)_3^-$ anion transformed into a number of different aluminate anions during the polymerization and then into a single anion structure near completion of the polymerization (Figure 1), indicative of the direct *anion involvement* in the polymerization.[13] These aluminate structures were identified to be free, noncoordinated anion $MeAl(C_6F_5)_3^-$ (**A**), MMA→$Al(C_6F_5)_3$ adduct (**B**, Figure 2), and enolaluminate anions Me(P)C═C-(OMe)$OAl(C_6F_5)_3^-$ (**C**, **D**).[14]

Second, low-temperature NMR studies reveal that the MMA-separated ion-pair **A** formed spontaneously upon mixing **2** and MMA equilibrates with **3** and **B** (eq 1) before the polymerization takes place. The origin of this key step, which results in a different

(1) For recent reviews, see: (a) Chum, P. S.; Kruper, W. J.; Guest, M. J. *Adv. Mater.* **2000**, *12*, 1759−1767. (b) Gladysz, J. A., Ed. *Chem. Rev.* **2000**, *100*, 1167−1682. (c) Marks, T. J.; Stevens, J. C., Eds. *Top. Catal.* **1999**, *7*, 1−208. (d) Britovsek, G. J. P.; Gibson, V. C.; Wass, D. F. *Angew. Chem., Int. Ed. Engl.* **1999**, *38*, 428−447. (e) Jordan, R. F., Ed. *J. Mol. Catal.* **1998**, *128*, 1−337. (f) McKnight, A. L.; Waymouth, R. M. *Chem. Rev.* **1998**, *98*, 2587−2598. (g) Piers, W. E. *Chem. Eur. J.* **1998**, *4*, 13−18. (h) Kaminsky, W.; Arndt, M. *Adv. Polym. Sci.* **1997**, *127*, 144−187. (i) Bochmann, M. *J. Chem. Soc., Dalton Trans.* **1996**, 255−270. (j) Brintzinger, H.-H.; Fischer, D.; Mülhaupt, R.; Rieger, B.; Waymouth, R. M. *Angew. Chem., Int. Ed. Engl.* **1995**, *34*, 1143−1170.

(2) For a recent review, see: Boffa, L. S.; Novak, B. M. in ref 1b, pp 1479−1493.

(3) Collins, S.; Ward, S. G. *J. Am. Chem. Soc.* **1992**, *114*, 5460−5462.

(4) Yasuda, H.; Yamamoto, H.; Yokota, K.; Miyake, S.; Nakamura, A. *J. Am. Chem. Soc.* **1992**, *114*, 4908−4909.

(5) Single-component cationic zirconocene systems: (a) Frauenrath, H.; Keul, H.; Höcker, H. *Macromolecules* **2001**, *34*, 14−19. (b) Cameron, P. A.; Gibson, V.; Graham, A. J. *Macromolecules* **2000**, *33*, 4329−4335. (c) Nguyen, H.; Jarvis, A. P.; Lesley, M. J. G.; Kelly, W. M.; Reddy, S. S.; Taylor, N. J.; Collins, S. *Macromolecules* **2000**, *33*, 1508−1510. (d) Stuhldreier, T.; Keul, H.; Höcker, H. *Macromol. Rapid Commun.* **2000**, *21*, 1093−1098. (e) Chen, E. Y.-X.; Metz, M. V.; Li, L.; Stern, C. L.; Marks, T. J. *J. Am. Chem. Soc.* **1998**, *120*, 6287−6305.

(6) Binary and ternary cationic zirconocene systems: (a) Shiono, T.; Saito, T.; Saegusa, N.; Hagihara, H.; Ikeda, T.; Deng, H.; Soga, K. *Macromol. Chem. Phys.* **1998**, *199*, 1573−1579. (b) Li, Y.; Ward, D. G.; Reddy, S. S.; Collins, S. *Macromolecules* **1997**, *30*, 1875−1883. (c) Deng, H.; Soga, K. *Macromolecules* **1996**, *29*, 1847−1848. (d) Deng, H.; Shiono, T.; Soga, K. *Macromolecules* **1995**, *28*, 3067−3073. (e) Deng, H.; Shiono, T.; Soga, K. *Macromol. Chem. Phys.* **1995**, *196*, 1971−1980. (f) Soga, K.; Deng, H.; Yano, T.; Shiono, T. *Macromolecules* **1994**, *27*, 7938−7940. (g) Collins, S.; Ward, D. G.; Suddaby, K. H. *Macromolecules* **1994**, *27*, 7222−7224. (h) Reference 3.

(7) For a theoretic study, see: Sustmann, R.; Sicking, W.; Bandermann, F.; Ferenz, M. *Macromolecules* **1999**, *32*, 4204−4213.

(8) (a) Nodono, M.; Tokimitsu, T.; Tone, S.; Makino, T.; Yanagase, A. *Macromol. Chem. Phys.* **2000**, *201*, 2282−2288. (b) Qian, C.; Nie, W.; Sun, J. *Organometallics* **2000**, *19*, 4134−4140. (c) Knjazhanski, S. Y.; Elizalde, L.; Cadenas, G.; Bulychev, B. M. *J. Polym. Sci. Part A: Polym. Chem.* **1998**, *36*, 1599−1606. (d) Giardello, M. A.; Yamamoto, Y.; Brard, L.; Marks, T. J. *J. Am. Chem. Soc.* **1995**, *117*, 3276−3277. (e) Boffa, L. S.; Novak, B. M. *Macromolecules* **1994**, *27*, 6993−6995. (f) Yasuda, H.; Yamamoto, H.; Yamashita, M.; Yokota, K.; Nakamura, A.; Miyake, S.; Kai, Y.; Kanehisa, N. *Macromolecules* **1993**, *26*, 7134−7143.

(9) (a) Sogah, D. Y.; Hertler, W. R.; Webster, O. W.; Cohen, G. M. *Macromolecules* **1987**, *20*, 1473−1488. (b) Webster, O. W.; Hertler, W. R.; Sogah, D. Y.; Farnham, W. B.; RajanBabu, T. V. *J. Am. Chem. Soc.* **1983**, *105*, 5706−5708.

(10) Bochmann, M.; Lancaster, S. J.; Hursthouse, M. B.; Malik, K. M. A. *Organometallics* **1994**, *13*, 2235−2243.

(11) Chen, E. Y.-X.; Kruper, W. J.; Roof, G.; Wilson, D. R. *J. Am. Chem. Soc.* **2001**, *123*, 745−746.

(12) (a) This feature is established by observing a further high-field shift in δ for *p*- and *m*-fluorines as well as the small $\Delta\delta$ ($\delta_m - \delta_p$) = 2.67 ppm in ^{19}F NMR chemical shifts of the anion.[12b,c] (b) Klosin, J.; Roof, G.; Chen, E. Y.-X.; Abboud, K. A. *Organometallics* **2000**, *19*, 4684−4686. (c) Horton, A. D.; de With, J.; van der Linder, A. J.; van de Weg, H. *Organometallics* **1996**, *15*, 2672−2674.

(13) The color changes observed during the polymerizations using **1** and **2** are also very different. See Supporting Information for details.

(14) For spectroscopic data for the free $MeAl(C_6F_5)_3^-$ anion and others, see ref 12b and Supporting Information.

10.1021/ja016188j CCC: $20.00
Published on Web 07/20/2001

Table 1. MMA Polymerization Results and Polymer Properties[a]

entry	initiator	T_p (°C)	t_p (h)	yield (%)	M_n [b]	M_w/M_n [b]	T_g [c] (°C)	[*rr*][d] (%)	[*mr*][d] (%)	[*mm*][d] (%)
1	*rac*-(SBI)ZrMe$^+$MeB(C$_6$F$_5$)$_3^-$	23	2	80	30 300	1.13	55.9	2.6	4.7	92.7
2	*rac*-(SBI)ZrMe$^+$MeAl(C$_6$F$_5$)$_3^-$	23	2	100	39 800	1.25	112.5	60.4	35.7	3.9
3	*rac*-(SBI)ZrMe$^+$MeAl(C$_6$F$_5$)$_3^-$	0	4	100	73 880	1.32	127.1	60.8	34.6	4.6
4	(i) B(C$_6$F$_5$)$_3$; (ii) *rac*-(SBI)ZrMe$_2$	23	2	80	28 440	1.12	54.7	3.1	6.5	90.4
5	(i) Al(C$_6$F$_5$)$_3$; (ii) *rac*-(SBI)ZrMe$_2$	23	2	85	28 770	1.19	110.5	60.6	35.1	4.3
6	Cp$_2$ZrMe$_2$ + B(C$_6$F$_5$)$_3$	23	1	100				66.7	30.8	2.5
7	Cp$_2$ZrMe$_2$ + Al(C$_6$F$_5$)$_3$	23	1	100				62.1	34.0	3.9
8	Me$_2$C(Cp)(Flu)ZrMe$_2$ + B(C$_6$F$_5$)$_3$	23	16	0						
9	Me$_2$C(Cp)(Flu)ZrMe$_2$ + Al(C$_6$F$_5$)$_3$	23	16	17				62.4	34.2	3.4
10	*rac*-Et(Ind)$_2$ZrMe$_2$ + B(C$_6$F$_5$)$_3$	23	2	100				1.2	2.8	96.0
11	*rac*-Et(Ind)$_2$ZrMe$_2$ + Al(C$_6$F$_5$)$_3$	23	2	100				60.2	35.8	4.0
12	^{t}BuLi	23	2	29	16 163	21.7		7.4	14.7	77.9
13	^{t}BuLi	−78	10	80	53 590	14.4		7.3	17.7	75.0
14	(i) 2Al(C$_6$F$_5$)$_3$; (ii) ^{t}BuLi	23	0.08	100	85 800	1.73	135.4	76.6	22.3	1.1
15	(i) 2Al(C$_6$F$_5$)$_3$; (ii) ^{t}BuLi	−78	4	84	59 800	1.33	**140.1**	**95.0**	5.0	0.0
16	(i) 2B(C$_6$F$_5$)$_3$; (ii) ^{t}BuLi	23	2	0						
17	Me$_2$C=C(OMe)OLi	23	2	52	14 695	18.8		10.7	22.5	66.8
18	Me$_2$C=C(OMe)OLi	−78	10	0						
19	(i) 2Al(C$_6$F$_5$)$_3$; (ii) Me$_2$C=C(OMe)OLi	23	0.08	100	52 100	**1.08**	127.2	78.4	20.6	1.0
20	(i) 2Al(C$_6$F$_5$)$_3$; (ii) Me$_2$C=C(OMe)OLi	−78	1.75	46	37 000	1.35	**138.1**	**94.2**	5.8	0.0
21	(i) 2B(C$_6$F$_5$)$_3$; (ii) Me$_2$C=C(OMe)OLi	23	2	0						

[a] Polymerization conditions: 46.7 μmol of initiator (I); mole ratio MMA/I = 200; 10 mL toluene; solvent/[M$_0$] = 10 v/v. [b] Determined by GPC relative to PMMA standards. [c] Determined by DSC from the second scan. [d] Determined by ^{1}H NMR spectroscopy.

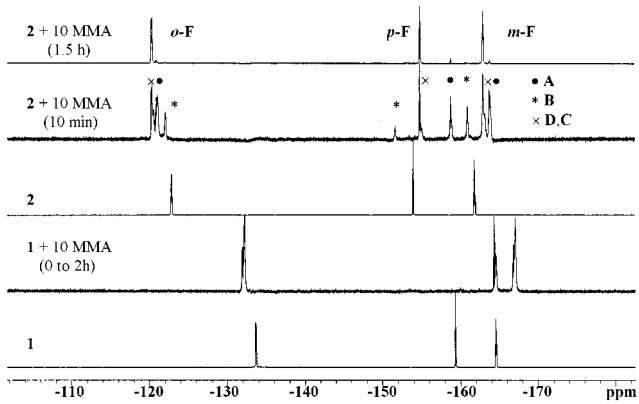

Figure 1. ^{19}F NMR spectra of various borate and aluminate anions involved in the polymerization in toluene-d_8.

initiation pathway for **2**, is attributable to the high Lewis acidity and oxophilicity of Al(C$_6$F$_5$)$_3$.[15]

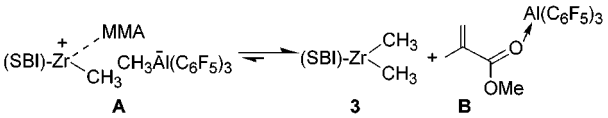

(1)

Third, "activated monomer" polymerization was carried out by adding **3** to the MMA activated by B(C$_6$F$_5$)$_3$ or Al(C$_6$F$_5$)$_3$ (runs 4 and 5). The same polymerization results were again obtained: the borane "activated monomer" polymerization produces isotactic PMMA while the alane "activated monomer" polymerization affords syndiotactic-rich PMMA.

Fourth, while polymer tacticity is very sensitive to the metallocene structure in MMA polymerizations activated with the borane (C_{2v}-metallocene, runs 6−7; C_s-metallocene, runs 8−9; C_2-metallocene, runs 10−11), stereospecificity of MMA polymerizations with the alane activation remains virtually unchanged upon variation of the metallocene structure.

Finally, highly active and syndiospecific polymerization systems are generated when the metallocenes are replaced with ^{t}BuLi and methyl lithioisobutyrate initiators. Thus, whereas polymerizations initiated by ^{t}BuLi or methyl lithioisobutyrate exhibit low activity and are predominately isotactic with broad molecular weight distributions (runs 12−13 and 17−18), addition of 2 equiv of the alane (one equiv. for generating enolaluminates and the other for activating monomer) brings about much faster and more controlled polymerization producing syndiotactic PMMA with tacticity ranging from moderate 76.6% to high 95.0% and T_g from 127.2 to high 140.1 °C and, M_w/M_n from 1.73 to 1.08, depending on polymerization temperature (runs 14−15 and 19−20). Interestingly, addition of the borane completely shuts down the polymerization (runs 16 and 21).

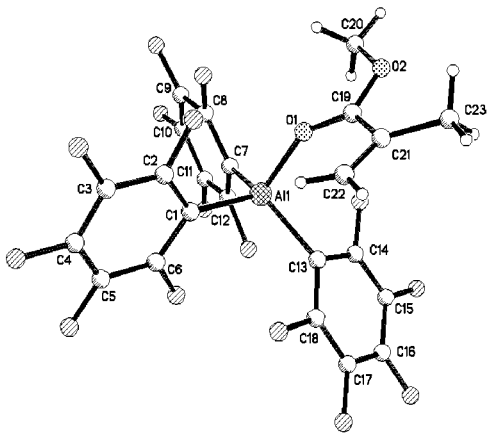

Figure 2. Crystallographic structure of MMA→Al(C$_6$F$_5$)$_3$ adduct. Selected bond lengths and angles (Å, deg): Al−O1 = 1.811(2); O1−C19 = 1.255(2); O2−C19 = 1.299(4); Al−O1−C19 = 148.2(2).

In summary, several lines of evidence reported here suggest a new polymerization pathway for metallocene-catalyzed polymerization of MMA which involves enolaluminates. In turn, studies of countercation affects lead to the efficient synthesis of highly syndiotactic PMMA. Further studies on kinetics and mechanistic details of the polymerization are in progress.

Supporting Information Available: Crystallographic data for Al(C$_6$F$_5$)$_3$·MMA, experimental details, spectroscopic data, representative NMR spectra, GPC traces (PDF). This material is available free of charge via the Internet at http://pubs.acs.org.

JA016188J

(15) This is also established by comparing $\Delta\delta$ ($\delta_{adduct} - \delta_{MMA}$) for CH$_3$O and CH$_3$ groups of the following adducts: B(C$_6$F$_5$)$_3$·MMA (−0.04, −0.09), (SBI)ZrMe$^+$·MMA (−0.13, −0.02), Al(C$_6$F$_5$)$_3$·MMA (−0.29, −0.57), suggesting the highest degree of activation by the alane in this series.